The Intermediate Barrier Performance of Electroless Co-W-B / Ni-P Stacked Deposits Between Cu and Solder Joint

Yoshihito Ii, Hiroki Okubo, Shoichi Fukui, Tetsuji Ishida, Shoji Iguchi, Katsuhisa Tanabe and Shigeo Hashimoto
C. Uyemura & Co., Ltd.
Osaka, Japan

ABSTRACT

Nickel (Ni) is one of the most common surface finishing materials for solder joint and wire bonding because it can behave as the diffusion barrier for Copper (Cu) and bring excellent reliability. Electroless Ni plating has many advantages such as high productivity, good thickness uniformity, and the deposition ability for isolated patterns of printed circuit boards without supplying electrolytic power. Electroless Ni plating is widely used as the jointing material for Tin (Sn) or Sn alloy solder in printed circuit boards, lead frames, and so on. The amorphous deposits of electroless Nickel-Phosphorus (Ni-P) generate the intermetallic compounds (IMC) with solder after the reflow and the remaining Ni behaves as the barrier between Cu and solder. In this time, the P amount of Ni-P deposits generally have the impact to the growth of IMC. Electroless Ni-P with high P (high P Ni) such as 10-12 wt% has been selected to achieve both corrosion resistance and solder joint reliability. Because the growth of Sn-Ni IMC between high P Ni is faster than deposits with lower P, the target thickness of high P Ni has been set to approximately 10 μm to sustain the Ni-P layer as the barrier layer between Cu and solder during reflow. However, if the Ni-Sn IMC is repeatedly formed and dissolved by the diffusion after solder jointing, the Ni-P layer reduces and finally disappears . As a result, an additional barrier layer is desirable for higher reliability. In this study, we investigated adding electroless Cobalt-Tungsten-Boron (Co-W-B) as a new intermediate barrier between Cu and solder jointing. We evaluated the bonding strength and IMC analysis after mounting Sn-Cu-Ni-P type solder on Cu/Co-W-B/Ni-P by using different reflow profiles. Results showed that Co-W-B 0.1-0.2 μm/Ni-P 1-2 μm stacked deposits had excellent bonding strength even though the Ni-P thickness is thinner such as 1 μm. After mounting solder, a P-rich layer was generated on the Co-W-B layer in cross-sectional Transmission Electron Microscope (TEM) observation. Scanning Transmission Electron Microscope (STEM) –Energy Dispersive X-ray Spectroscopy (EDS, STEM-EDS) analysis showed the P-rich layer and Co-W-B layer prevented diffusion between solder and Cu. Furthermore, even if after the thermal loading of high temperature, the bonding strength was excellent. Additionally, the cross-section analysis of STEM-EDS revealed that a thin layer composed of Ni, Co and P was formed between Co-W-B and the P-rich layer. This thin layer also might behave as the barrier for solder. In conclusion, Co-W-B / Ni-P stacked deposits exhibited excellent reliability as the additional intermediate barrier layer between Cu and solder.

Key words: Electroless Co-W-B, Electroless Ni-P, barrier metal, solder joint

INTRODUCTION

Ni is used as the surface finishing material for solder jointing widely because it can make intermetallic compounds with solder and provides excellent bonding strength[1,2]. Especially, electroless Ni has benefits as the aspect of productivity or deposition ability for isolated pads without electrolytic power supply. Electroless Ni deposits generally include co-deposited P and this P content has effects for solder jointing.

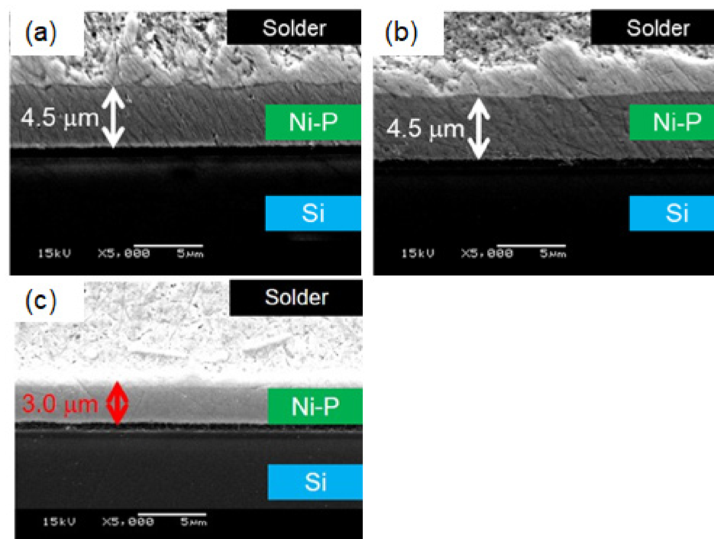

Figure 1: Typical cross-sectional SEM image after soldering with Ni-P 5 μm deposits which have each P amount (5k). (a) P 2-4 wt.%(Low P), (b) P 6-8 wt.% (middle P) and (c) P 10-12 wt.%(High P). The solder is a Tin-Silver-Copper (Sn-Ag- Cu) type and soldering under 280 °C, 8 min reflow.

Figure 1 shows high P Ni has faster consumption thickness by the solder joint compared with Low P or Middle P type deposits due to much affinity to the solder[3]. However, high P Ni has excellent corrosion resistance properties. Therefore, the target thickness is set thicker such as 10 μm for the solder jointing application using corrosion resistant high P Ni so that a barrier between Cu and solder can remain.

On the other hand, electroless Co-W-B deposits were evaluated for the thermal diffusion barrier of the semiconductor Cu wiring in some papers[4-6]. According to these studies, it demonstrated the barrier ability under 400 °C[5].

Based on this background, we investigated to add a Co-W-B layer between Cu and high P Ni as the intermediate barrier between Cu and solder.

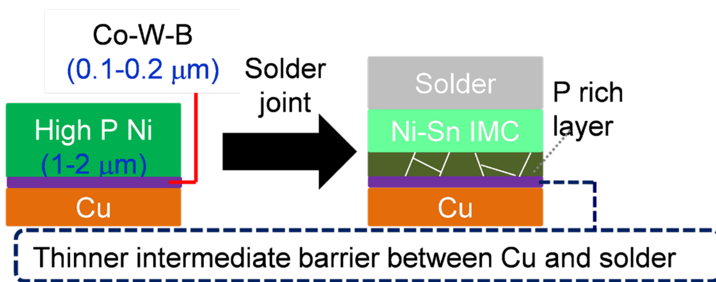

Figure 2: Co-W-B / high P Ni stacked deposit and after solder joint structure.

Figure 2 shows our proposal in this investigation. The Co-W-B is anticipated to act as the stronger and thinner barrier instead of high P Ni. The high P Ni thickness could be thinner because it is only needed for generating the IMC with solder.

In this study, we evaluated the bonding strength, the barrier ability, and detailed cross sectional structural analysis after solder jointing with Co-W-B / high P Ni stacked deposits.

EXPERIMENTAL

In this investigation, C1100P Cu test pieces were used as the substrates. The Cu test pieces were plated using the process below.

Table 1: Electroless Co-W-B / high P Ni plating process

Process	chemical	temp (°C)	Time (min)
Cleaner	Mild acid type	50	3
Micro etching	100 g/L SPS	25	1
Acid rinse	10% H_2SO_4	r.t.	1
E-less Co-W-B	W:35-65wt.%/B: 0-0.2 wt.%	73	16(for 0.1 μm)
E-less Ni	High P type(P 10-12wt.%)	90	4(for 1.0 μm)

In this process, the Palladium (Pd) activation wasn't needed for the Cu substrate because dimethylamine borane (DMAB) which was in the electroless Co-W-B chemical as the reducer had catalytic ability on Cu surfaces and it allowed deposits on Cu directly. The Co-W-B deposit or Co-W-B / high P Ni deposition status was evaluated by Focused Ion Beam Scanning Electron Microscope (FIB-SEM, XVision 210 DB, Hitachi high-tech). Moreover, elemental analysis of the Co-W-B deposit was performed by Auger Electron spectroscopy (AES, JAMP-9500F, JEOL).

The plated test pieces were solder jointed with Sn-Cu-Ni-P type solder by below Figure 3 (a) or (b) condition respectively under N2-formic acid atmosphere.

One of the purposes for this Co-W-B / Ni-P stacked deposits is to apply for the automotive electronics which high melting point solder is generally used for solder jointing. Therefore, these high temperature reflows which were shown in Figure 3 (a) or (b) were chosen for this investigation even though it can work under the low temperature reflow.

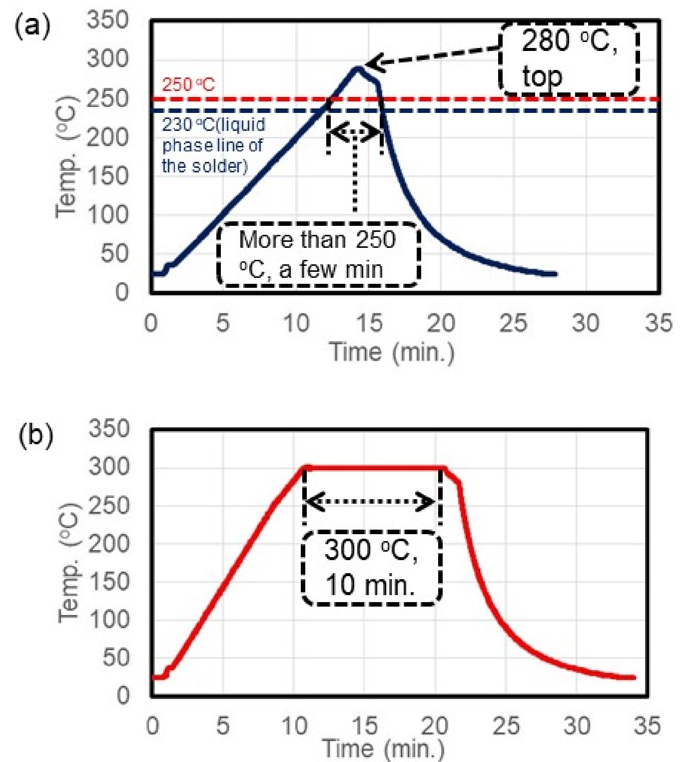

Figure 3: Reflow profiles for soldering with Co-W-B / high P Ni (a) 280 °C, top (b) 300 °C, 10 min.

After solder joining with a nut which was coated with electro Ni on iron (ϕ 5 mm) by the above reflow conditions, these were evaluated for bonding strength and fracture mode by the load tester (MODEL-1311VC, AIKOH ENGINEERING). Moreover, the plating test pieces with mounted solder were evaluated for the cross-sectional status by Scanning Electron Microscope (SEM, JSM-7800F, JEOL). The detailed structural analysis and elemental analysis was performed by Transmission Electron Microscope (TEM, JEM-F200, JEOL) and attached Energy Dispersive X-ray Spectroscopy detector (EDS, JED-2300T, JEOL).

Cross-section polishing for SEM was performed by ion milling system (IM-4000, Hitachi high-tech). The TEM specimen preparation was performed by FIB-SEM (XVision 210 DB, Hitachi high-tech).

RESULTS AND DISCUSSION

Preparation of electroless Co-W-B or Co-W-B / high P Ni deposit

The electroless Co-W-B deposit was deposited directly on Cu. Figure 4 shows the cross-sectional backscattered electron (BSE) image of Co-W-B deposit and its AES depth profile analysis.

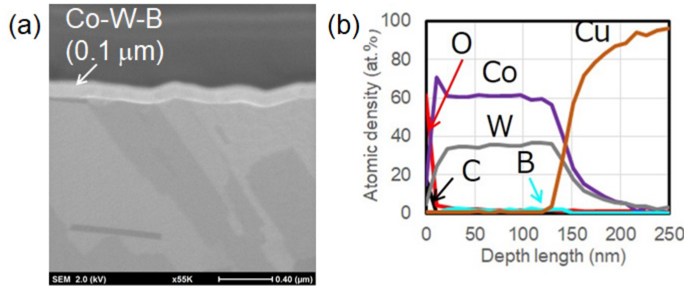

Figure 4: The deposition status and elemental analysis of Co-W-B deposit. (a) The cross-sectional BSE image (55k) (b) AES depth profile analysis.

Figure 4 (a) shows uniform deposition of Co-W-B without any defects such as voids. Figure 4 (b) shows the W and B content in Co-W-B deposit. Based on Figure 4 (b), the Co, W, B contents value, which was 54 nm for the depth length were Co:63.4 at.%, W:34.86 at.%, and B:1.74 at.% respectively. Therefore, these values were Co: 36.76 wt.%, W: 63.05 wt.% and B: 0.20 wt.%.

Moreover, Figure 5 is the cross-sectional BSE image of Co-W-B / high P Ni stacked deposits. It also shows that high P Ni could deposit on Co-W-B properly.

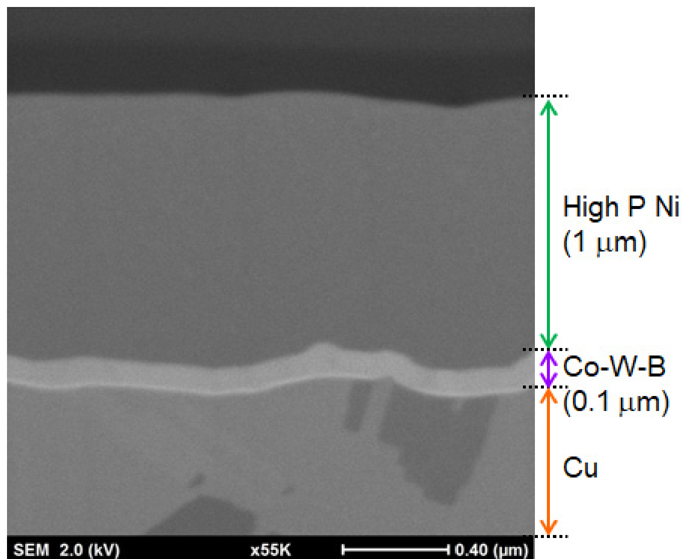

Figure 5: The cross-sectional BSE image of Co-W-B / high P Ni stacked deposits (55k).

The evaluation of the bonding strength

First of all, the bonding strength and its fracture mode in the various deposits after soldering with Figure 3 reflow profile was evaluated by the nut pull test. The procedure is illustrated in Figure 6.

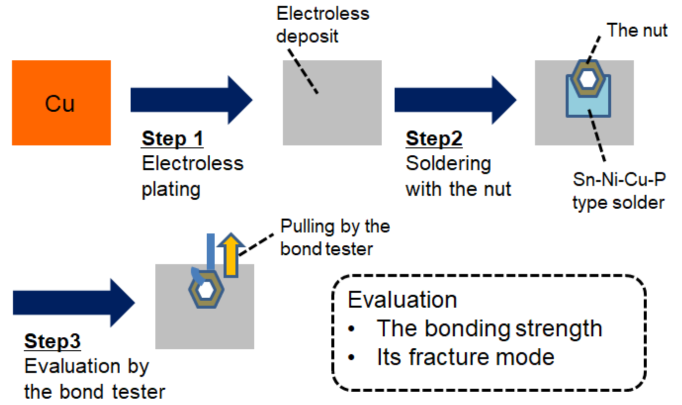

Figure 6: The nut pull test procedure

The list of electoless deposits, applied reflow profile for solder joint and evaluation results are shown in Table 2.

Table 2: The list of electroless deposits, reflow profile which used for solder jointing and the evaluation result of bonding strength by the average of three tests.

leg	Co-W-B (μm)	High P Ni (μm)	Reflow profile for solder joint	Bonding strength (N)				fracture
				N1	N2	N3	Ave.	
1	0	10	280 °C top	875	1003	930	936	solder
2	0	1		--	487	382	435	solder/Cu
3	0.2	1		1117	936	939	997	solder
4	0.2	1	300 °C, 10 min	908	791	1032	910	solder

The thicker high P Ni single deposit showed excellent bonding strength, however thinner such as 1 μm thickness of high P Ni single deposit was unable to keep the bonding strength and fractured between solder and Cu.

However, when 0.2 μm of Co-W-B deposit was added between Cu and 1 μm of high P Ni deposit, the bonding strength showed improvement. Moreover, these stacked deposits kept excellent bonding strength and good fracture mode despite applying harder reflow profile which is shown Figure 3 (b). In conclusion, adding the Co-W-B layer was effective in keeping excellent bonding strength under thinner high P Ni conditions.

The evaluation of the IMC generation and cross-sectional status

To confirm the jointing status between high P Ni and solder, these solder mounted test pieces were analyzed by cross-sectional SEM observation.

Figure 7 shows the cross-sectional BSE image which was mounted solder on high P Ni 10 μm deposit by 280 °C, top reflow condition which was shown in Figure 3 (a).

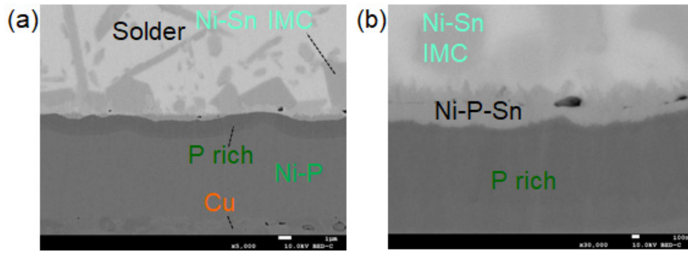

Figure 7: The cross-sectional BSE image of solder mounted on high P Ni 10 μm deposits (a): Low magnification (5k), (b) High magnification (30k).

This was the typical structure of the solder jointing with high P Ni. One can see the Ni-P-Sn reaction layer and P-rich layer generation on the remaining high P Ni layer. The high P Ni thickness was 8 μm and acted as the barrier between Cu and solder. Therefore, Sn couldn't contact Cu and brought excellent bonding strength.

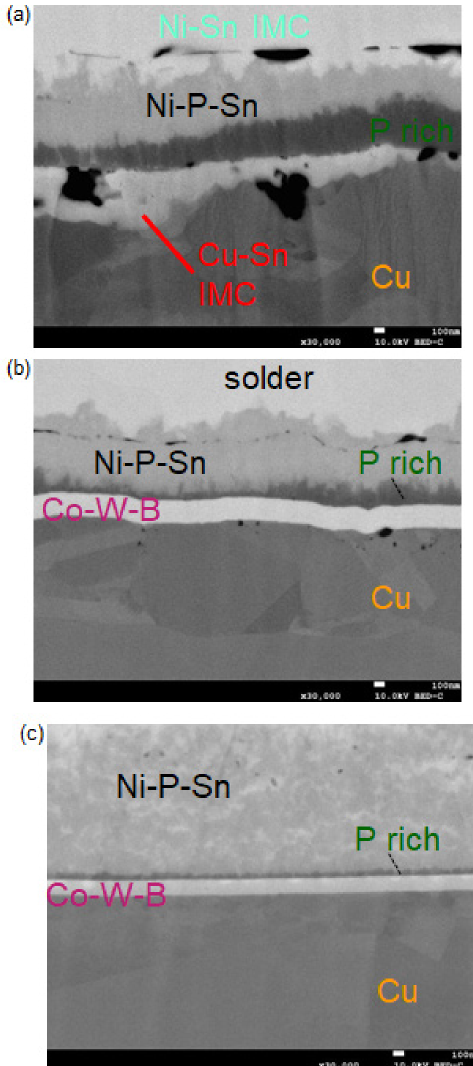

Figure 8: The cross-sectional BSE image of solder mounted on high P Ni 1 μm deposit with or without 0.2 μm of Co-W-B deposits (30k). (a) Without 0.2 μm of Co-W-B deposits (b) With 0.2 μm Co-W-B (c) With 0.2 μm Co-W-B and soldering under harder reflow.

Figure 8 (a) shows the cross-sectional BSE image of solder mounted with high P Ni 1 μm in jointing by 280 °C, top reflow temperature. This image shows the Cu-Sn IMC generated between the P-rich layer and Cu. Therefore, the bonding strength was poorer than high P Ni 10 μm condition. On the other hand, Figure 8 (b) shows Co-W-B 0.2 μm / high P Ni 1 μm stacked deposits with solder jointing with 280 °C, top reflow temperature. It shows a P-rich layer connected on Co-W-B directly and there was no Cu-Sn IMC generated due to the Co-W-B layer. Moreover, Figure 8 (c) is the cross-sectional image applied harder Figure 3 (b) reflow profile. It showed 0.2 μm Co-W-B deposits withstood as the barrier between Cu and solder under harder reflow such as 300 °C, 10 min. Figure 8 (c) and (b) show differences structurally.

The detail structural and elemental analysis comparison of the solder mounted on Co-W-B / high P Ni stacked deposit jointing with different reflow conditions.

Based on Figure 8 (b) and (c), there were differences structurally by reflow condition. Therefore, it might be that they had a different Ni-Sn IMC generation status.

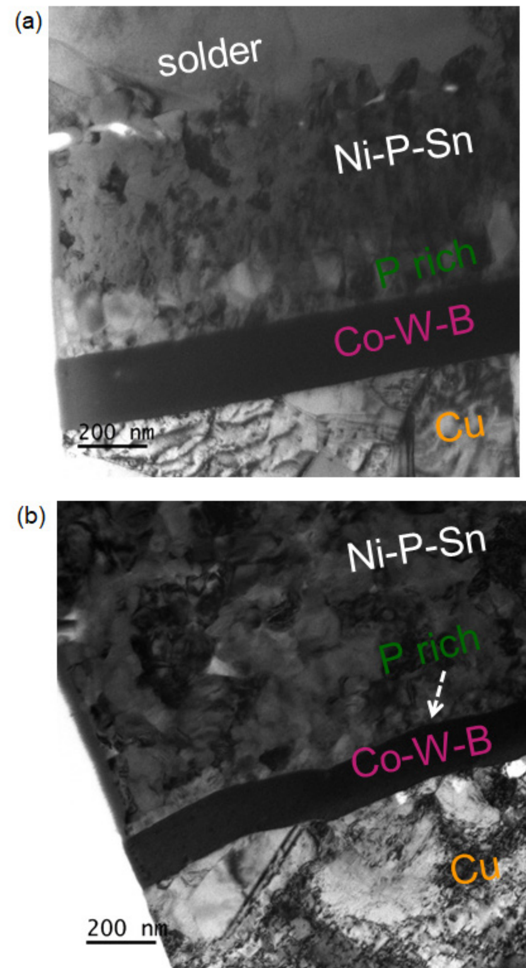

Figure 9: The cross-sectional TEM image of the solder mounted with different reflow profile on Co-W-B 0.2 μm / Ni-P 1 μm stacked deposit. (a) Solder joint with 280 °C, top reflow. (b) Solder joint with 300 °C, 10 min. reflow.

Figure 9 (b) shows a thinner P-rich layer than Figure 9 (a). Therefore, the IMC generation reaction proceeded between P rich layer and IMC under harder reflow.

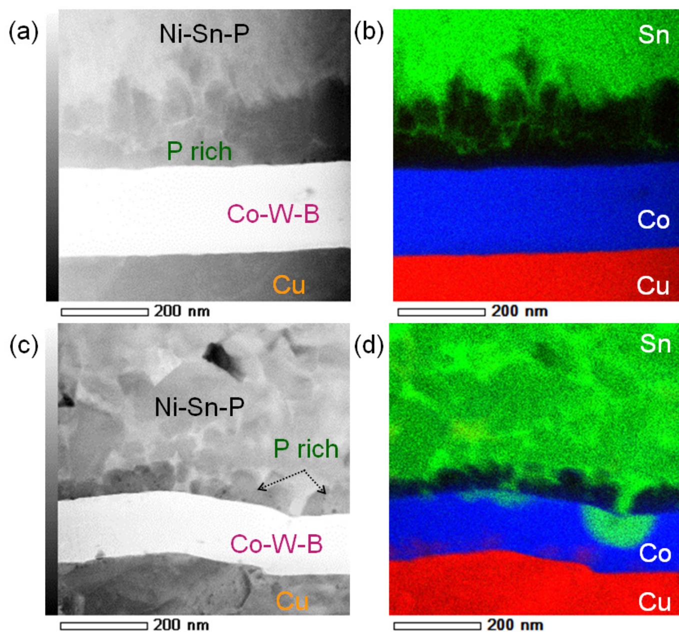

Figure 10: Cross-sectional High-Angle Annular Dark Filed Scanning Transmission Electron Microscope (HAADF -STEM) image and correspondence EDS overlap mapping with Sn, Co and Cu element. (a) HAADF -STEM image of solder joint with 280 °C, top reflow. (b) EDS map of Figure 10 (a). (c) HAADF-STEM image of solder joint with 300 °C, 10 min. reflow. (d) EDS map of Figure 10 (c)

Figure 10 shows HAADF-STEM image and correspondence EDS map overlapped with Sn, Co and Cu to evaluate the diffusion barrier status between Cu and solder. Figure 10 (b) shows that the solder diffusion was prevented by P- rich layer. On the other hand, Cu diffusion was prevented Co-W-B layer. In Figure 10 (d) the indicated Cu diffusion was still prevented by Co-W-B deposit. Moreover, Sn diffusion proceeded along the grain boundary of the P-rich layer and connected to Co-W-B layer. However, Sn diffusion was prevented inside of Co-W-B layer and didn't connect to Cu even though harder reflow conditions were applied. Consequently, Co-W-B and P-rich layer acted as the double barrier between Cu and solder.

High temperature storage test of Co-W-B / high P Ni stacked deposit after solder joint.

Co-W-B / high P Ni stacked deposit with solder jointing specimen was subjected to the high temperature storage test (HTST) to evaluate the thermal durability. The evaluation sample was plated Co-W-B 0.1 µm / high P Ni 1.0 µm and solder jointing with Sn-Cu-Ni-P type solder by Figure 3 (a) reflow. Table 3 shows temperature and aging time conditions in HTST and the evaluation result of bonding strength and fracture mode by the nut pull test.

Table 3: HTST temperature, aging time condition and the result of bonding strength by nut pull test which evaluated by the average of three tests.

time (h) at 175 °C	Bonding strength (N)				fracture
	N1	N2	N3	Ave.	
0	1176	936	939	997.3	solder
250	903	713	875	830.3	solder
500	988	1074	766	942.7	solder
100	808	758	749	771.7	solder

Based on the above evaluation, Co-W-B / high P Ni stacked deposit kept excellent bonding strength and fracture mode throughout this HTST test. Moreover, Figure 11 shows a cross-sectional BSE image of the specimen which passed each aging time.

Figure 11: The cross-sectional BSE image of the specimen which passed each aging time. (a) 0 h, (b) 250 h (c) 500h (d) 1000 h. Magnification: 30k.

Figure 11 shows there wasn't generation of the Sn-Cu IMC and Co-W-B acted as intermediate barrier between Cu and solder throughout HTST test. However, thinner P-rich area was generated and expanded gradually. It has possibility to proceed the diffusion reaction between P-rich layer and solder.

The detail cross-sectional observation and elemental analysis of thinner P-rich layer area.

In Co-W-B / high P Ni stacked deposit, the P-rich layer generated after solder jointing acted as the barrier for Sn diffusion. On the other hand, the thinner P-rich area expanded gradually in the evaluation of the HTST. This thinner P-rich area was generated by the reaction proceeding between the P-rich layer and the solder. To identify the detail of this reaction proceeding, cross-sectional TEM observation and elemental analysis by EDS was performed using the specimen which was kept for 1000h, at 175 °C in HTST.

Figure 12 shows the cross-sectional TEM image of HTST 175 °C, 1000 h specimen. Figure 12 (a) exhibited thinner P-rich area and (b) showed thicker P-rich area. Co-W-B layer of both areas didn't change the status and Cu diffusion was prevented. On the other hand, the Ni-P-Sn reaction layer was expanding in the thinner P-rich layer area. Moreover, it seemed like the Ni-P-Sn reaction layer was proceeding along with the grain boundary of the P-rich layer and stopped on the thinner new crystalline layer which was generated on the Co-W-B layer.

This thinner new crystalline layer on the Co-W-B layer didn't generate a thicker P-rich layer area. Therefore, it had the possibility to generate new IMC by the reaction proceeding between the P-rich layer and solder.

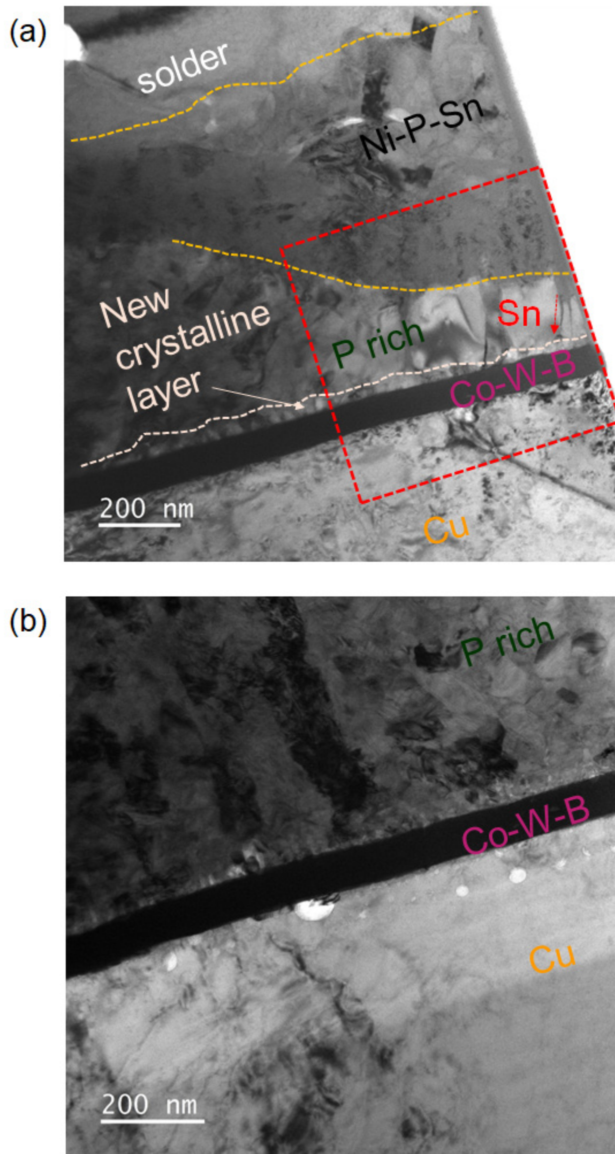

Figure 12: The cross-sectional TEM image of the HTST 1000 h aging of Co-W-B / high P Ni stacked deposit with solder jointing (a) thinner P-rich area (b) thicker P-rich area

To clarify the generation root of a new crystalline layer in the thinner P-rich layer area, EDS analysis was performed. Figure 13 shows the HAADF-STEM image and EDS Co mapping analysis data. Figure 13 (a) is the HAADF-STEM image of the thinner P rich layer area while (b) is its Co mapping data. Figure 13 (a) also shows the Ni-P-Sn reaction layer was proceeding along with the grain boundary of the P-rich layer and stopping on the new crystalline layer alike TEM image. Figure 13 (b) shows that Co was diffused to P-rich layer from Co-W-B in the thinner P-rich area. Therefore, this data indicated the new crystalline layer was including Co and one of its generation root was Co diffusion.

On the other hand, Figure 13 (c) shows the HAADF-STEM image of the thicker P-rich layer area and 13 (d) is its EDS Co mapping data. In Figure 13 (d), Co diffusion was not proceeding so much compared to the thinner P-rich layer area.

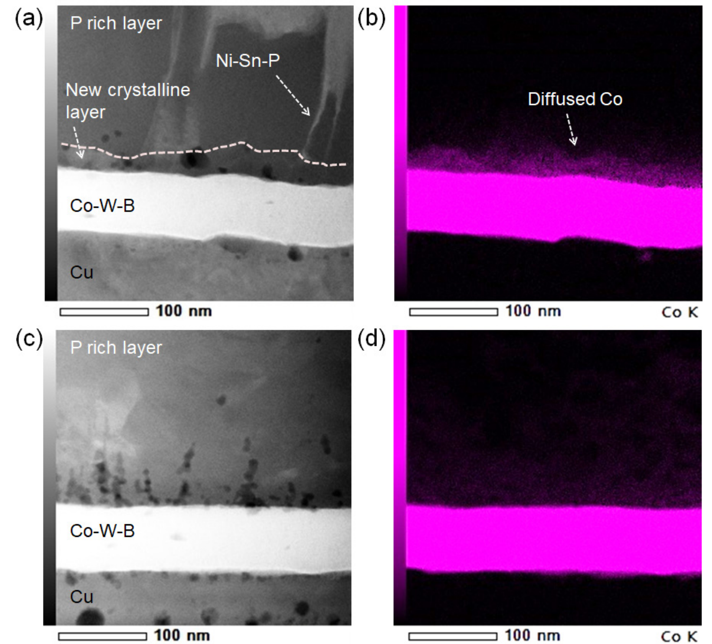

Figure 13: Cross-sectional HADDF-STEM image of the thinner P-rich area or thicker P-rich area and EDS Co map (a) HADDF-STEM image of the thinner P-rich area (b) EDS map of Figure 13 (a) (c) HADDF-STEM image of thicker P-rich area (d) EDS map of Figure 13 (b).

In order to observe and identify the composition of the new crystalline layer on the Co-W-B layer, Bright Filed Scanning Transmission Electron Microscope (BF -STEM) observation and EDS quantitative analysis of this layer were performed in Figure 14.

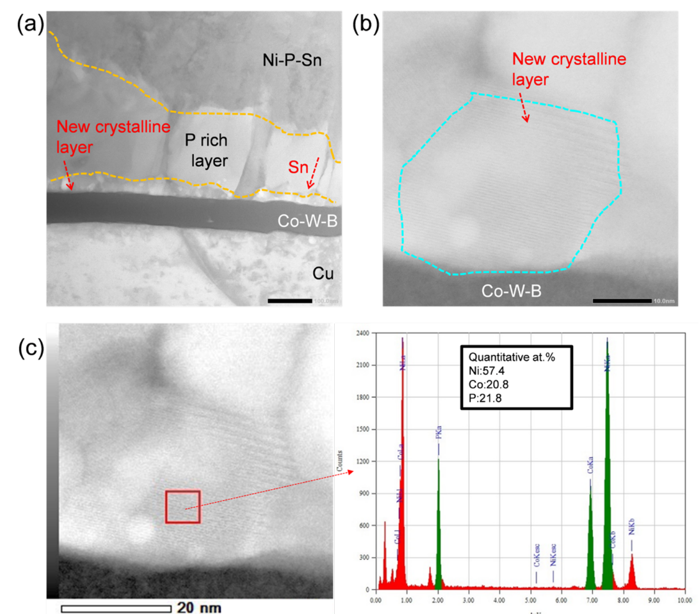

Figure 14: Cross-sectional BF-STEM image of the thinner P-rich area and EDS Quantitative analysis of the new crystalline layer. (a) Low magnification of the BF-STEM image (b) High magnification of the BF-STEM image (c) EDS spectrum and Quantitative analysis.

Figure 14 (a) shows the low magnification image of BF-STEM in the thinner P-rich layer area and (b) shows the high magnification image of the new crystalline layer on Co-W-B layer. Figure 14 (b) shows the lattice fringe and grain boundary in the new crystalline layer. Therefore, this data indicated the layer is a crystalline structure. Figure 14 (c) is the EDS quantitative analysis result of this grain. Based on Figure 14 (c), this new crystalline layer consists of Ni, P, and Co. and the quantitative value was Ni:57.4 at.%, Co: 20.8 at.% and P :21.8 at.% respectively. Overall, this new Ni-Co-P IMC was generated by the Co diffusion to the P-rich layer and it also worked as the barrier for the solder diffusion.

Figure 15 illustrates the estimated mechanism of the Ni-Co-P IMC generation at the thinner P-rich layer area. The reaction between Ni and Sn is generally uneven. Therefore, it is possible to proceed a reaction between Ni and Sn partially. Moreover, the Co diffusion from Co-W-B layer proceeded at the area which Ni and Sn reaction proceeded faster. Consequently, the Ni-Co-P IMC was generated.

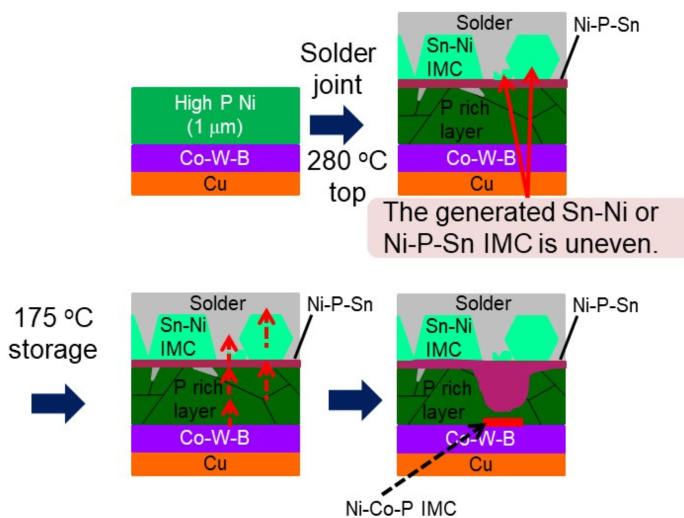

Figure 15: Estimated mechanism of the Ni-Co-P IMC generation at the thinner P rich layer area.

CONCLUSIONS

In this investigation, adding the 0.1 - 0.2 µm of electroless Co-W-B deposits between Cu and high P Ni for the barrier was examined. The following examination was performed: the bonding strength, structural and elemental analysis, and conducting of the HTST.

Based on this investigation, Co-W-B / high P Ni stacked deposits showed excellent bonding strength and Co-W-B prevented the Cu-Sn IMC generation. In structural and elemental analysis, thin high P Ni on the Co-W-B deposits was exchanged to Ni-Sn IMC and P-rich layer after solder joint. Moreover, Co-W-B and the P-rich layer acted as the double barrier between Cu and solder. Furthermore, the new Co-Ni-P IMC was generated at thinner P-rich layer areas. It also acted as the barrier for solder.

Figure 16 shows the investigation summary of Co-W-B / high P Ni stacked deposit for the solder joint. Overall, the Co-W-B deposit acted as the thinner and stronger thermal diffusion barrier for Cu. Moreover, the P-rich layer which was exchanged from high P Ni on Co-W-B deposit acted as the barrier for solder. To use this stacked deposit, high P Ni thickness could be reduced to 1 µm from 10 µm.

In this investigation this new Co-W-B / Ni-P stacked deposits for solder joint was mainly evaluated as the aspect of the thermal durability.

We'll evaluate the extended thermal cycling test as the aspect of durability for the combination of thermal and stress as the next step.

We believe these stacked deposits will provide a benefit for space saving for the packaging and downsizing of electronic devices.

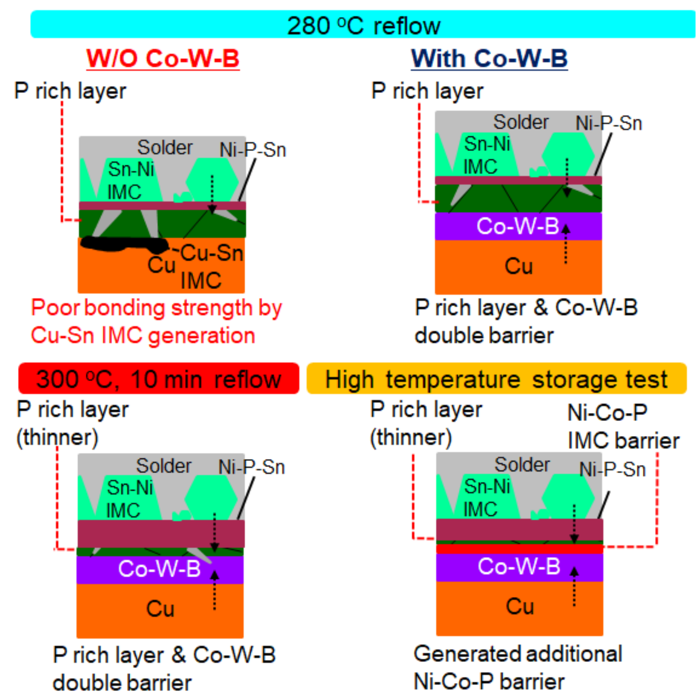

Figure 16: The investigation summary of Co-W-B / high P Ni stacked deposit for the solder joint reliability.

REFERENCES

1. Chi-Won Hwang, Katsuaki Suganuma, Masayuki Kiso and Shigeo Hashimoto, "Interface microstructures between Ni-P alloy plating and Sn-Ag-(Cu) lead free solders", J. Mater. Res., 2003, 18, (11), 2540

2. Yukinori Oda, Masayuki Kiso, Seigo Kurosaka, Akira Okada, Kota Kitajima and Shigeo Hashimoto, "Study of Suitable Palladium and Gold Thickness in ENEPIG Deposits for Lead Free Soldering and Gold Wire Bonding", 41st International Symposium on Microelectronics, Providence, RI, 2008.

3. Yasunori Chonan, Takao Komiyama, and Jin Onuki, "Reliability and Interfacial Structures of Solder Joint Between Lead Free Solder and Electroless Plated Ni-P Alloy Film", Hyomen Gijutsu, 2003, 54, (2), 30

4. Vadim Bogush, Yelena Sverdlov, Hila Einati, Arulkumar Shanmugasundram, Timothy Weidman and Yosi Shacham-Diamand, "Microstructure and material properties of electroless Co(W, B) thin film", Advanced Metallization Conference proceeding, 2004, 843

5. H. Nakano, T. Itabasi, and H. Akahoshi, "Electroless Deposited Cobalt-Tungsten-Boron Capping Barrier Metal on Damascene Copper Interconnection", J. Electrochem. Soc., 2005, 152, (3), C163

6. Hyo-Chol Koo, Sung Ki Cho, Oh Joong Kwon, Myung-Won Suh, Young Im and Jae Jeong Kim, "Improvement in the Oxidation Resistance of Cu Films by an Electroless Co-Alloy Capping Process", J. Electrochem. Soc., 2009, 156, (7), D236

BIOGRAPHIES

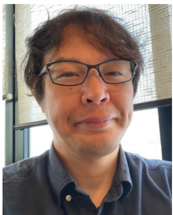

Yoshihito Ii is working for the R&D division in C. Uyemura & Co., Ltd. as an engineer. He received his master's degree at Graduate School of Natural Science and Technology in Okayama University. He developed some electroless plating or pretreatment chemicals and submitted some patents with his co-workers. He recently studied the diffusion barrier ability of electroless Co-W-B deposits for Cu and gave presentations in some conferences in Japan.

Hiroki Okubo is an engineer at the R&D division of C. Uyemura & Co., Ltd.

Shoichi Fukui is a sales staff at Nagoya branch of C. Uyemura & Co., Ltd.

Tetsuji Ishida is a section director at R&D divison of C. Uyemura & Co., Ltd.

Shoji Iguchi is a section director at the techinical suport group in Nagoya branch of C. Uyemura. & Co., Ltd.

Katsuhisa Tanabe is a manager at R&D divison of C. Uyemura & Co., Ltd.

Shigeo Hashimoto is a senior managing director at C. Uyemura & Co., Ltd.